Study on DFIG Dissipation Energy Model and Low-Frequency Oscillation Mechanism Considering the Effect of PLL

Yaqi Shen, Jing Ma, *Senior Member, IEEE*, and Letian Wang

***Abstract*—Considering the dynamic characteristics of phase-locked loop (PLL), the effect of interaction between doubly fed induction generator (DFIG) and power grid on system low-frequency oscillation is revealed from the perspective of dissipation energy. First, the dynamic energy model of DFIG with PLL is derived, and the component that varies nonperiodically is extracted and defined as the dissipation energy. Second, the dissipation energy is decomposed into the free dissipation energy and DFIG-grid coupled dissipation energy. On this basis, the free dissipation intensity and coupled dissipation intensity are defined, which, respectively, characterize the immanent damping of DFIG and the DFIG-grid interaction degree. Thus, the contribution degree of DFIG to electromechanical oscillation is quantified for evaluation, and the mechanism of interaction between DFIG and power grid is further revealed. Finally, hardware-in-the-loop simulation tests with real-time digital simulator of the IEEE 10-machine 39-bus system verify that when the oscillation frequency of PLL is close to electromechanical oscillation frequency, strong coupling and resonance exist between DFIG and grid, and negative dissipation effect on the oscillation of DFIG will result. Thus, DFIG, as an oscillator, continuously injects dynamic energy to the grid, causing the system to oscillate to instability.**

***Index Terms*—Doubly fed induction generator (DFIG) energy model, dissipation energy, low-frequency oscillation, phase-locked loop (PLL).**

NOMENCLATURE

DFIG	Doubly fed induction generator.
PLL	Phase-locked loop.
Δ	Small increment of a variable.
$\Delta\theta_s$	Variation of phase angle of DFIG voltage at grid-connecting point.
$\Delta\theta_{pll(1)}$	PLL free response component.
$\Delta\theta_{pll(2)}$	PLL forced response component.
ΔW	Dynamic energy, energy change during oscillation.
K_i	Integration gain of PI control link in PLL.
K_p	Proportion gain of PI control link in PLL.
Ω_0	Oscillation amplitude of phase angle of voltage at PCC.
r	Oscillation attenuating coefficient of phase angle of voltage at PCC.
ω_m	Oscillation frequency of phase angle of voltage at PCC.
s	Stator side.
0	Initial value.
d, q	d-axis and q-axis in synchronous rotating speed.
r_1, r_2	Eigenvalues of small-signal model of PLL.
D	Nonperiodical component item.
α	Free attenuation coefficient of phase-locked angle when PLL excites oscillation mode.
β	Free oscillation frequency of PLL phase-locked angle.
ΔW^D	Dissipation energy, aperiodic component of dynamic energy.
ΔE	Energy dissipation intensity.
ΔE_{couple}	DFIG-grid coupled dissipation intensity.
ΔE_{free}	Free dissipation intensity.

Manuscript received January 2, 2019; revised April 12, 2019 and July 20, 2019; accepted September 3, 2019. Date of publication September 10, 2019; date of current version January 10, 2020. This work was supported in part by the National Key Research and Development Program of China under Grant 2018YFB0904003, in part by the National Natural Science Foundation of China under Grant 51777070, in part by Chinese Universities Scientific Fund under Grant 2018JQ01, and in part by Chinese Universities Scientific Fund under Grant 2018ZD01. Recommended for publication by Associate Editor Y. A.-R. I. Mohamed. *(Corresponding author: Jing Ma.)*

Y. Shen, J. Ma, and L. Wang are with the State Key Laboratory of Alternate Electrical Power System with Renewable Energy Sources, North China Electric Power University, Beijing 102206, China (e-mail: jsntsyq1994@163.com; hdmajing@163.com; ncepu_wanglt@163.com).

Color versions of one or more of the figures in this article are available online at http://ieeexplore.ieee.org.

Digital Object Identifier 10.1109/TPEL.2019.2940522

I. INTRODUCTION

DUE to the weak coupling between the stator and rotor of DFIG, DFIG will exhibit weak damping characteristics after disturbance occurs in the system. The introduction of PLL stabilizes DFIG integration voltage, but also strengthens the coupling between DFIG and power grid; thus, the participation of DFIG in system electromechanical oscillation increases, which may aggravate system damping level and even intimidate the safe and stable operation of power grid [1]–[5]. Therefore, it is urgent to study how the coupling between DFIG and power grid affects system low-freqeuncy oscillation.

Currently, research on low-freqeuncy oscillation of the system with wind power integration mainly applies the state matrix method and the damping torque method [6]–[12]. The state matrix method reveals the mechanism in which the wind turbines affect system stability by tracing back to the influencing factors of system state matrix. In [13], the effect of factors such as

DFIG integration scale, operation mode, etc., on system state matrix is anlayzed, and conclusion is reached that traditonal wind turbines change system state matrix by affecting system power flow, but do not introduce any new electromechanical oscillation mode. Chondrogiannis and Barnes [14] point out that different integration locations of wind turbines may improve system oscillation mode, but may also aggravate system damping. In [15], the coupling between DFIG and synchronous generator is analyzed from the perspective of PLL dynamic characteristic using the state matrix method, and it is found out that PLL is the key link that affects DFIG low-freqeuncy oscillation. The damping torque method traces the correlation between control parameters and oscillation modes by adjusting control parameters and anlayzing the corresponding effect on the damping torque. Du *et al.* [16] analyze the effect of DFIG dynamic characteristic on system damping using the damping torque method and points out that DFIG is approximately decoupled from the grid. Lv *et al.* [17] reveal the mechanism in which the control link of DFIG affects the oscillation mode of two-generator system using the damping torque method. The above references all analyze the effect of wind power integration on system low-freqeuncy oscillation from the perspective of power grid, with the conclusion that there exists oscillation mode coupling between wind turbines and power grid, which may affect system damping level. However, the above methods need to use state variables of all the generators in the system, and most research on the coupling between wind turbines and power grid is qualitative analysis. There is still a lack of illustration on the quantification of wind generator-grid coupling degree and the mechanism in which wind generator-grid coupling results in system oscillatory instability.

The essence of wind generator-grid coupling is the transmission of energy between wind generator and power grid. Thus, by excavating the wind generator-grid energy transmission information during system oscillation, a method to analyze low-freqeuncy oscillation of system with DFIG integration based on the dissipation energy model is proposed in this article. First, the dynamic energy model of DFIG with PLL is established, and the nonperiodical component is extracted and defined as the dissipation energy. On this basis, the DFIG dissipation energy is decomposed into the free dissipation energy which is determined by DFIG parameters and the dissipation energy which is generated by DFIG-grid coupling. And then, by defining the free dissipation energy intensity and coupled dissipation energy intensity, the damping contribution degree of DFIG to electromechanical oscillation is evaluated, and the participation degree of DFIG in electromechanical oscillation is quantified. Furthermore, the physical process of DFIG-grid energy interaction causing the system to oscillate to instability is depicted, and the mechanism in which DFIG-grid coupling affects system low-frequency oscillation is illustrated. Finally, hardware-in-the-loop simulation tests are conducted in real-time digital simulator (RTDS) of the IEEE 10-machine 39-bus system, and comparison is made between eigenvalue analysis and the proposed method, which verifies the correctness and effectiveness of the proposed method.

II. Dynamic Energy Model of DFIG With PLL

A. DFIG Port Dynamic Energy Function

The energy function of the power system can be constructed based on the node current equation. For any system, extract the imaginary part of the node current equation and do integral operation, so that the following energy function as shown in (2) can be constructed:

$$\boldsymbol{I_{in}} = \boldsymbol{Y}\boldsymbol{U}_B - \boldsymbol{I}_G + \boldsymbol{I}_L \tag{1}$$

$$W = \int \mathrm{Im}(((\boldsymbol{Y}\boldsymbol{U}_B - \boldsymbol{I}_G + \boldsymbol{I}_L)^*)^T d\boldsymbol{U}_B) \tag{2}$$

where $\boldsymbol{Y}$ is system admittance matrix, and $\boldsymbol{U}_B$ is the column vector of bus voltages. $\boldsymbol{I}_G$ and $\boldsymbol{I}_L$ are, respectively, the column vector of injection current at generator nodes and the column vector of injection current at load nodes. Im means extracting the imaginary part of the complex.

Extract the energy of generator in (2)

$$\int \mathrm{Im}(I_{Gi}^* dU_i). \tag{3}$$

The energy function based on the node current equation is universal for all generators. However, due to the different internal structures, the detailed expression of energy function varies. Considering the power system with DFIG, (3) is transformed to the *dq*-axis, i.e.,

$$\begin{aligned} W &= \int \mathrm{Im}\left((-I_G^*)\, dU\right) \\ &= -\left[\int P_e d\theta + \int I_d dU_q - \int I_q dU_d\right] \end{aligned} \tag{4}$$

where P_e is the generator output active power. θ is the angular difference between *xy*-axis and *dq*-axis, which can also represent the phase-locked angle of PLL. U_d, U_q, I_d, and I_q are, respectively, the *d*-axis and *q*-axis components of voltage and current at the output terminal of generator. *W* is the injection energy from grid to generator.

According to Lyapunov's second stability criterion, if the variation of system overall energy V ($V > 0$) with time $\dot{V}$ is constantly negative, system overall energy will keep decreasing until it reaches the minimum value, i.e., the equilibrium state, and the system is stable. Otherwise, system overall energy will keep increasing, and the system will go unstable.

According to (2), system overall energy is composed of three parts—generator energy, line energy, and load energy. When a certain generator in the system exports energy in the oscillation process and causes the dynamic energy at the terminal of this generator ΔW to keep increasing, this generator has positive effect on the increasing of system overall energy *V*. According to Lyapunov's second stability criterion, this generator will lower system stability level and exert negative damping effect on system oscillation. Conversely, when a certain generator in the system absorbs energy in the oscillation process and causes the dynamic energy at the terminal of this generator ΔW to keep decreasing, this generator has negative effect on the increasing

of system overall energy V. According to Lyapunov's second stability criterion, this generator will improve system stability level and exert positive damping effect on system oscillation. Therefore, if DFIG absorbs energy, which means the energy change during oscillation $\Delta W > 0$, DFIG has positive damping effect on the oscillation. If DFIG exports energy, $\Delta W < 0$ and DFIG has negative damping effect on the oscillation. In this article, the energy change during oscillation is defined as *dynamic energy,* denoted as ΔW.

Variables in (4) are expressed by changes in relative steady-state values and DFIG dynamic energy function can be described as

$$\begin{aligned}\Delta \boldsymbol{W}_{\mathrm{DFIG}} = & \int \left(\Delta I_d + I_{d0}\right) d\left(\Delta U_q + U_{q0}\right) \\ & - \left(\Delta I_q + I_{q0}\right) d\left(\Delta U_d + U_{d0}\right) \\ & + \int \left(\Delta P_e + P_{e0}\right) d\left(\Delta\theta + \theta_0\right) \\ = & \int \Delta I_d d\Delta U_q - \Delta I_q d\Delta U_d + \int \Delta P_e d\Delta\theta \\ & + \int I_{d0} d\Delta U_q - I_{q0} d\Delta U_d + \int P_{e0} d\Delta\theta \quad (5)\end{aligned}$$

where 0 represents state values of variables.

Denote

$$\begin{cases}\Delta W^O_{\mathrm{DFIG}} = \int I_{d0} d\Delta U_q - I_{q0} d\Delta U_d + \int P_{e0} d\Delta\theta \\ \Delta W^D_{\mathrm{DFIG}} = \int \Delta I_d d\Delta U_q - \Delta I_q d\Delta U_d + \int \Delta P_e d\Delta\theta.\end{cases} \quad (6)$$

When oscillation occurs, $\Delta W^O_{\mathrm{DFIG}}$ is a component varying periodically with time and does not affect the variation trend of energy. $\Delta W^D_{\mathrm{DFIG}}$, containing nonperiodical components, is the main concern of this article.

It can be seen from (6), $\Delta W^D_{\mathrm{DFIG}}$ contains two energy parts: ΔW_1 and ΔW_2, which can be expressed as

$$\Delta W_1 = -\int \Delta I_d d\Delta U_q + \int \Delta I_q d\Delta U_d \quad (7)$$

$$\Delta W_2 = -\int \Delta P_e d\Delta\theta \quad (8)$$

where ΔW_1 is the dynamic energy component directly affected by the output voltage and current of DFIG, and ΔW_2 is the dynamic energy component directly affected by the active power and phase-locked angle.

B. Dynamic Energy Component Directly Affected by the Output Voltage and Current of DFIG ΔW_1

The structure of DFIG integrated with the power system is shown in Fig. 1. The reactance of DFIG transmission line is *L*.

When low-frequency oscillation with frequency of ω_d occurs in the DFIG-integrated power system, the amplitude of current oscillation component is $I_n e^{\gamma t}$. The *d*–axis and *q*–axis components of current at DFIG grid-connecting point are expressed as

$$\begin{aligned}\Delta i_d &= I_n e^{\gamma t} \cos\left[\left(\omega_s - \omega_d\right) t + \varphi_i\right] \\ \Delta i_q &= -I_n e^{\gamma t} \sin\left[\left(\omega_s - \omega_d\right) t + \varphi_i\right]\end{aligned} \quad (9)$$

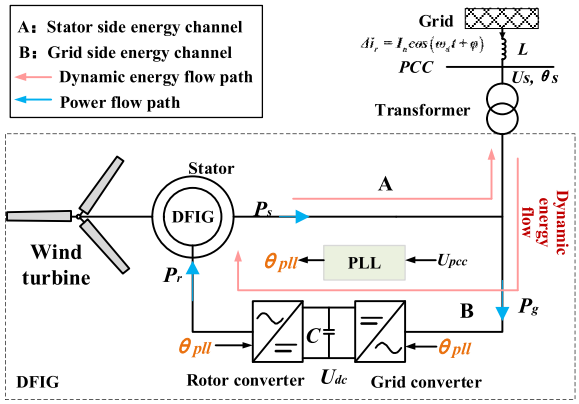

Fig. 1. Model of DFIG integrated with power system and energy channel.

where φ_i is the phase of current oscillation component, and γ is the attenuation coefficient of system low-frequency oscillation amplitude.

Considering the effect of PLL, the low-frequency component of voltage at the grid-connecting point can be expressed as (after *dq-abc* transformation)

$$\begin{aligned}\Delta u_d &= U_n e^{\gamma t} \cos\left[\theta_{\mathrm{pll}} - \omega_d t + \varphi_u\right] \\ \Delta u_q &= -U_n e^{\gamma t} \sin\left[\theta_{\mathrm{pll}} - \omega_d t + \varphi_u\right]\end{aligned} \quad (10)$$

where $\theta_{\mathrm{pll}} = \omega_s t + \Delta\theta_{\mathrm{pll}}$. φ_u is the phase of voltage oscillation component, $\varphi_u = \varphi_i + \varphi_L$. φ_L is the impedance angle of DFIG output transmission line, $\varphi_L = \arctan\frac{\omega_d L}{R}$.

Apply (9) and (10) to (4), so that the expression of ΔW_1 can be obtained

$$\begin{aligned}\Delta W_1 = & -I_n U_n e^{2\gamma t} \sin\left(\Delta\theta_{\mathrm{pll}} + \varphi_u - \varphi_i\right) \\ & - \int I_n U_n e^{2\gamma t} \cos\left(-\Delta\theta_{\mathrm{pll}} + \varphi_i - \varphi_u\right)\omega_d dt. \quad (11)\end{aligned}$$

It can be seen from (11) that phase-locked angle $\Delta\theta_{\mathrm{pll}}$ will affect dynamic energy component ΔW_1 by affecting the values of U_d and U_q.

C. Dynamic Energy Component Directly Affected by the Active Power and Phase-Locked Angle ΔW_2

Since the stator side is directly connected to power grid, there are two energy channels between DFIG and system. The DFIG output power can be expressed as

$$P_e = P_s - P_g \quad (12)$$

where P_s and P_g are, respectively, the stator-side output electromagnetic power, and the grid power absorbed by the grid-side converter.

In this article, it is assumed that the capacitance of dc bus is big enough; thus, the transient process of dc bus can be neglected [15]. Apply (12) to (8), so that ΔW_2 can be further described as

$$\Delta W_2 = -\int \left(\Delta P_s + \Delta P_g\right) d\Delta\theta_{\mathrm{pll}} \quad (13)$$

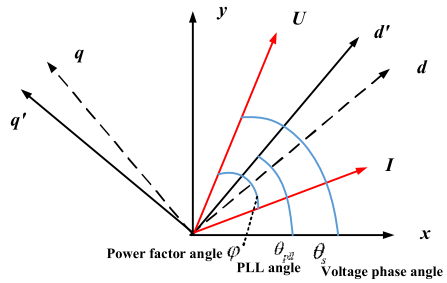

Fig. 2. Voltage and current phasor diagram of stator side under incomplete tracking.

When PLL does not track perfectly, the diagram of DFIG stator-side voltage and current phasors is shown in Fig. 2, where *d'q'*-axis represents the position of *dq*-axis considering the dynamic process of PLL, the rotating speed of which is $\omega_{\rm pll} \neq \omega_s$. The phase-locked angle is $\theta_{\rm pll}$, the phase angle of stator voltage is θ_s, and the angle between voltage and current, i.e., the power factor angle is φ.

The error of output active power generated by PLL can be expressed as

$$P_{\rm err} = U_s I_s \cos\left(\theta_s - \theta_{\rm pll} + \varphi\right) - U_s I_s \cos\varphi. \tag{14}$$

Linearization of (14) yields

$$\begin{aligned}\Delta P &= \Delta P_s + \Delta P_g \\ &= -U_s I_s \sin\left(\theta_{s0} - \theta_{\rm pll0} + \varphi\right)\left(\Delta\theta_s - \Delta\theta_{\rm pll}\right) \\ &\quad - U_g I_g \sin\varphi\left(\Delta\theta_s - \Delta\theta_{\rm pll}\right)\end{aligned} \tag{15}$$

where $\Delta\theta_s$ is the variation of phase angle of DFIG voltage at the grid-connecting point. $\Delta\theta_{\rm pll}$ is the variation of phase-locked angle. φ is the power factor.

Consider that the voltage and current of the grid-side converter are much smaller than the voltage and current of stator-side converter, and the reactive power provided by the grid-side converter is next to 0, i.e., $U_g I_g \sin\varphi \approx 0$; thus, the last item in (15) is next to 0, and the variation of dynamic energy caused by the grid-side converter can be neglected. The dynamic energy of DFIG is mainly generated by the stator side, i.e.,

$$\Delta P \approx \Delta P_s = -U_s I_s \sin\left(\theta_{s0} - \theta_{\rm pll0} + \varphi\right)\left(\Delta\theta_s - \Delta\theta_{\rm pll}\right). \tag{16}$$

Apply (16) to (8), the dynamic energy caused by PLL can be expressed as

$$\begin{aligned}\Delta W_2 = &\int U_s I_s \sin\left(\theta_{s0} - \theta_{\rm pll0} + \varphi\right)\Delta\theta_s d\Delta\theta_{\rm pll} \\ &- \frac{1}{2} U_s I_s \sin\left(\theta_{s0} - \theta_{\rm pll0} + \varphi\right)\Delta\theta_{\rm pll}^2.\end{aligned} \tag{17}$$

It can be seen from (17) that the dynamic energy caused by PLL is determined by the deviation value of phase-locked angle $\Delta\theta_{\rm pll}$ and the deviation value of bus power angle during electromechanical oscillation $\Delta\theta_s$.

In this article, a three-phase synchronous PLL is adopted, which is widely used at present. The linearized model of PLL can be expressed as

$$\frac{d^2\Delta\theta_{\rm pll}}{dt^2} + K_p U_s \frac{d\Delta\theta_{\rm pll}}{dt} + K_i U_s \Delta\theta_{\rm pll} = K_i U_s \Delta\theta_s \tag{18}$$

where U_s is DFIG stator voltage. $\Delta\theta_{\rm pll}$ is PLL output phase angle, and K_p and K_i are, respectively, the proportional gain and integral gain of PLL control.

After disturbance occurs, the dynamic characteristic of the phase angle of DFIG integration voltage can be expressed as

$$\Delta\theta_s = \Omega_0 e^{rt} \cos\left(\omega_m t + \varphi_c\right) \tag{19}$$

where Ω_0 is the initial amplitude of the phase angle of bus voltage. r is the attenuation coefficient of the phase angle of bus voltage. ω_m is the frequency of electromechanical oscillation. φ_c is the phase shift caused by disturbance.

According to the structure of solution to (18), the dynamic characteristics of PLL are composed of a free response, which is only decided by PLL parameters, and a forced response decided by system oscillation modes

$$\Delta\theta_{\rm pll} = \Delta\theta_{\rm pll(1)} + \Delta\theta_{\rm pll(2)} \tag{20}$$

$$\begin{cases}\Delta\theta_{\rm pll(1)} = C_1 e^{r_1 t} + C_2 e^{r_2 t} & 4K_i \leq K_p^2 U_s \\ \Delta\theta_{\rm pll(1)} = e^{\alpha t}\left(C_1 \cos\beta t + C_2 \sin\beta t\right) & 4K_i > K_p^2\end{cases} \tag{21}$$

$$\Delta\theta_{\rm pll(2)} = e^{rt}\left(b\cos\omega_m t + d\sin\omega_m t\right) \tag{22}$$

where $\Delta\theta_{pll(1)}$ is the free response, which can be further divided into PLL exciting oscillation mode and not exciting oscillation mode based on different PLL parameters. r_1 and r_2 are two eigenvalues of $\Delta\theta_{pll(1)}$, β is the oscillation mode of PLL, and α_1 is the attenuation coefficient of this oscillation mode. C_1 and C_2 are coefficients determined by the initial values of the phase-locked angle and rotating speed. The expression of the parameters are shown as (A-1) and (A-2). Considering r_1, r_2, $\alpha < 0$, the free response of PLL will not diverge or go unstable. $\Delta\theta_{pll(2)}$ is the forced response. b and d are the constants decided by $\Delta\theta_s$ and PLL parameters, which can be expressed as (B-1) and (B-2) in Appendix B.

Apply (20) to (17), so that

$$\begin{aligned}\Delta W_2 = &\int U_s I_s \sin\left(\theta_{s0} - \theta_{\rm pll0} + \varphi\right)\Delta\theta_s d\left(\Delta\theta_{\rm pll(1)} + \Delta\theta_{\rm pll(2)}\right) \\ &- \frac{1}{2} U_s I_s \sin\left(\theta_{s0} - \theta_{\rm pll0} + \varphi\right) \\ &\times \left(\Delta\theta_{\rm pll(2)}^2 + 2\Delta\theta_{\rm pll(1)}\Delta\theta_{\rm pll(2)}\right) \\ &- \frac{1}{2} U_s I_s \sin\left(\theta_{s0} - \theta_{\rm pll0} + \varphi\right)\Delta\theta_{\rm pll(1)}^2.\end{aligned} \tag{23}$$

The first two items in (23), related to the forced response of PLL $\Delta\theta_{pll(2)}$, reflect the energy coupling between DFIG and system. It is denoted as DFIG-grid coupled energy $\Delta W_{\rm couple}$. The last term is only related to the free response of PLL $\Delta\theta_{pll(1)}$ and characterizes the immanent damping effect of PLL. It is denoted as free response energy $\Delta W_{\rm free}$

$$\begin{aligned}\Delta W_{\rm couple} = &\int U_s I_s \sin\left(\theta_{s0} - \theta_{\rm pll0} + \varphi\right) \\ &\Delta\theta_s d\left(\Delta\theta_{\rm pll(1)} + \Delta\theta_{\rm pll(2)}\right) \\ &- \frac{1}{2} U_s I_s \sin\left(\theta_{s0} - \theta_{\rm pll0} + \varphi\right) \\ &\times \left(\Delta\theta_{\rm pll(2)}^2 + 2\Delta\theta_{\rm pll(1)}\Delta\theta_{\rm pll(2)}\right)\end{aligned}$$

$$\Delta W_{\rm free} = -\frac{1}{2} U_s I_s \sin\left(\theta_{s0} - \theta_{\rm pll0} + \varphi\right)\Delta\theta_{\rm pll(1)}^2. \tag{24}$$

It can be seen from (24), PLL parameters influence the coupling between DFIG and system and system stablity, as a result. The following sections will analyze the effect of PLL parameters in detail.

III. Low-Frequency Oscillation Mechanism of Interaction Between DFIG and Power System by Dynamic Energy

Cumulative process of dynamic energy reflects the damping effect of DFIG on low frequency oscillation. In order to quantitatively analyze the effect, dissipation energy and dissipation intensity index are defined in this article. By analyzing the dissipation intensity function that contains PLL dynamic equation, the mechanism of how the DFIG-grid coupling caused by PLL affects low-frequency oscillation can be further revealed.

A. Definition of Dissipation Energy and Dissipation Intensity

Apply (21) and (22) to (23), so that the dynamic energy caused by PLL can be expressed in the following form:

$$\Delta W_2 = f\left(e^t\right) + g\left(\sin\omega_m t\right) \tag{25}$$

where $f(e^t)$ is the aperiodic component associated with e^t, and $g(\sin\omega_m t)$ is the periodic component associated with the oscillation frequency.

For (25), take the variation in an oscillation period *T*. ΔW_2 can be approximated as

$$\Delta W_2|_{\Delta t=T} \approx a\Delta t \tag{26}$$

where *a* is the average gradient of $f(e^t)$ during the oscillation period *T*.

It can be seen from (26), the variation of periodic component $g(\sin\omega_m t)$ is zero during oscillation period *T* and the aperiodic component $f(e^t)$ is the leading component which characterizes the variation trend of the dynamic energy. When the variation of $f(e^t)$ is positive, DFIG absorbs dynamic energy and positively damps system oscillation; when the variation of $f(e^t)$ is negative, DFIG emits dynamic energy and deteriorates system damping. Thus, $f(e^t)$ characterizes the dissipation process of dynamic energy in the system, and is defined as *dissipation energy*, denoted asΔW^D.

Moreover, the variation of $\Delta W_2|_{\Delta t=T}$ is approximately linear during the period *T*, and its gradient is *a*. If $a > 0$, $\Delta W_2|_{\Delta t=T}$ is positive and its value increases with the increasing of *a*. That is to say, the dynamic energy dissipated by DFIG per unit time increases, and the system oscillation is suppressed faster than before. Thus, the value of *a* characterizes the degree of absorption of energy by DFIG. This article defines the variation of nonperiodical component of energy per unit time *a* as the *dissipation intensity* of energy, which is denoted as ΔE. The definition of ΔE is

$$\Delta E = \frac{d\Delta W^D}{d\Delta t}. \tag{27}$$

The bigger the ΔE, the stronger the damping effect of DFIG on system oscillation; and the smaller the ΔE, the weaker the damping effect of DFIG on system damping. If ΔE turns negative, DFIG will exhibit negative damping and continuously inject dynamic energy to the system, causing the system to go unstable.

According to the definition of dissipation intensity in (27), the dissipation intensity corresponding to two energy components in (24) are, respectively, DFIG-grid coupled dissipation intensity and free dissipation intensity, denoted as ΔE_{couple} and ΔE_{free}, which, respectively, characterize the damping effect of coupling between DFIG and grid on system oscillation and the damping effect of PLL free response.

B. DFIG Energy Dissipation Intensity Analysis Under Different PLL Parameters

The dynamic characteristics of PLL contain two cases: PLL not exciting oscillation mode and PLL exciting oscillation mode. In this section, the influence of DFIG on dissipation intensity is analyzed under the two cases, and the energy interaction between PLL and system is explored. On this basis, the mechanism of PLL inducing low frequency oscillation instability is illuminated.

1) PLL Not Exciting Oscillation Mode: When PLL does not excite any oscillation mode, in the expression of ΔW_1, PLL free response will generate nonperiodical component, so that $\sin(\Delta\theta_{\text{pll}} + \varphi_u - \varphi_i)$ and $\cos(\Delta\theta_{\text{pll}} + \varphi_u - \varphi_i)$ will also contain nonperiodical components. As for the value of $\Delta\theta_{\text{pll}} + \varphi_u - \varphi_i$, consider that $\varphi_u - \varphi_i = \varphi_L$, i.e., line impedance angle, and for long-distance DFIG output transmission line, $R \ll X_L$, thus $\varphi_L \approx 90^\circ$. Meanwhile, according to the dynamic characteristic equation of PLL, when PLL does not excite any oscillation mode, the free response of $\Delta\theta_{\text{pll}}$ is the superposition of two attenuating exponents which rapidly decreases to 0 after a small decline; thus, $\Delta\theta_{\text{pll}} \ll \varphi_L$. Based on the above analysis, when PLL does not excite any oscillation mode, $\sin(\Delta\theta_{\text{pll}} + \varphi_u - \varphi_i)$ and $\cos(\Delta\theta_{\text{pll}} + \varphi_u - \varphi_i)$ are mainly determined by φ_L, i.e.,

$$\sin\left(\Delta\theta_{\text{pll}} + \varphi_u - \varphi_i\right) \approx \sin\left(\varphi_L\right)$$
$$\cos\left(\Delta\theta_{\text{pll}} + \varphi_u - \varphi_i\right) \approx \cos\left(\varphi_L\right) \approx 0.$$

Apply the above approximation to (11), so that

$$\Delta W_1 = -I_n U_n e^{2\gamma t} \sin\left(\varphi_L\right). \tag{28}$$

It can be seen from (28) that, when PLL does not excite any oscillation mode, ΔW_1 will generate nonperiodical component, i.e., dissipation energy, which is the coupled energy that system-side oscillation generates in DFIG. This dissipation energy is only affected by the amplitudes of system-side oscillation current and voltage and does not vary as PLL parameters vary.

Apply (28) to (27), so that the dissipation intensity generated by ΔW_1, i.e., $\Delta E_{\text{couple1}}$ can be obtained

$$\Delta E_{\text{couple1}} = -2\gamma I_n U_n e^{2\gamma t}. \tag{29}$$

This article is mainly focused on the mechanism in which the coupling between DFIG and grid causes system oscillation to diverge. When the amplitudes of oscillation components of voltage and current generated by disturbance in the system gradually

attenuate, $\gamma < 0$, and the dissipation intensity that system oscillation generates at the terminal of DFIG $\Delta E_{\text{couple1}} > 0$; thus, this dissipation intensity will accelerate the converging of system oscillation. When the amplitudes of oscillation components of voltage and current generated by disturbance in the system gradually diverge, $\gamma > 0$, and the dissipation intensity that system oscillation generates at the terminal of DFIG $\Delta E_{\text{couple1}} < 0$, thus this dissipation intensity will aggravate system oscillation.

In the expression of ΔW_2, considering PLL not exciting any oscillation mode, there is no coupling between $\Delta\theta_s$ and $\Delta\theta_{pll(1)}$. Thus, $\int \Delta\theta_s d\Delta\theta_{\text{pll}(1)}$ is a periodical component and does not affect the increase or decrease of energy. In this case, DFIG-grid coupled dissipation intensity is only determined by the force response of PLL.

Apply the first item in (21) and (23) to (24) and (27), coupling dissipation intensity and free dissipation intensity can be obtained

$$\begin{aligned}\Delta E_{\text{free}} &= -\frac{1}{2}U_s I_s \sin\left(\theta_{s0} - \theta_{\text{pll}0} + \varphi\right) \\ &\quad \times \left(2rC_1^2 e^{2r_1 t} + 2(r_1 + r_2)C_1 C_2 e^{(r_1+r_2)t}\right) \\ &\quad - \frac{1}{2}U_s I_s \sin\left(\theta_{s0} - \theta_{\text{pll}0} + \varphi\right) 2r_2 C_2^2 e^{2r_2 t} \\ \Delta E_{\text{couple}} &= \frac{1}{4}U_s I_s \sin\left(\theta_{s0} - \theta_{\text{pll}0} + \varphi\right) e^{2rt} \\ &\quad \times \frac{\left(r^2 + \omega_m^2\right)\left[r - (r_1 + r_2)\right]}{A^2 + B^2} \end{aligned} \tag{30}$$

where

$$\begin{aligned} A &= r^2 - (r_1 + r_2)\, r + r_1 r_2 - \omega_m^2 \\ B &= \omega_m \left[2r - (r_1 + r_2)\right]. \end{aligned}$$

It can be seen from (20), since $r, r_1, r_2 < 0$, the free dissipation intensity ΔE_{free} is constantly positive. Considering $K_p U_s = -(r_1 + r_2)$ and $K_i U_s = r_1 r_2$, the value of ΔE_{free} increases as K_i increases and decreases as K_p increases.

The value of coupling intensity ΔE_{couple} is determined by r and $r_1 + r_2$. When $r < r_1 + r_2$, $\Delta E_{\text{couple}} > 0$ and the coupling between DFIG and grid has positive damping on oscillation. In this case, the value of ΔE_{couple} increased as K_i increases and decreases as K_p increases. When PLL parameters meet the condition that $0 > r > r_1 + r_2$, $\Delta E_{\text{couple}} < 0$ and coupling between DFIG and grid negatively damps the oscillation. However, in this case, $e^{2rt} \ll e^{r_1 + r_2}$. Namely, the free dissipation plays the leading role and the total dissipation intensity keeps positive. DFIG exhibits positive damping to the oscillation.

It should be noted that the overall dissipation intensity of DFIG is composed of $\Delta E_{\text{couple1}}$ (generated by ΔW_1) and ΔE_{free} and $\Delta E_{\text{couple2}}$ (generated byΔW_2). Consider that during low-frequency oscillation, the oscillation amplitudes of current and voltage I_n and U_n are both much smaller than the amplitudes of power-frequency current and voltage I_s and U_s; thus, the value of $\Delta E_{\text{couple1}}$ is much smaller than the values of ΔE_{free} and $\Delta E_{\text{couple2}}$, and the overall dissipation intensity of DFIG is determined by the sum of ΔE_{free} and $\Delta E_{\text{couple2}}$.

Based on the above analysis, when PLL not exciting oscillation mode, the dissipation intensity of DFIG keeps positive, and increase as K_i increases, while decreases as K_p increases. With this PLL parameters setting, DFIG exhibit positive damping on the force and free response caused by system oscillation.

2) PLL Exciting Oscillation Mode: In the expression of ΔW_1, since $\Delta\theta_{\text{pll}}$ varies periodically with time, $\sin(-\Delta\theta_{\text{pll}} + \varphi_i - \varphi_u)$ and $\cos(-\Delta\theta_{\text{pll}} + \varphi_i - \varphi_u)$ in ΔW_1 are also periodically time varying, i.e., ΔW_1 will not generate any new dissipation energy and dissipation intensity components. As a result, when PLL excites oscillation mode, the dynamic energy component directly affected by the output voltage and current of DFIG ΔW_1 will not affect the damping level of DFIG concerning low-frequency oscillation.

In the expression of ΔW_2, when the frequency of PLL free response differs considerably from the frequency of system low frequency oscillation, there is weak coupling between $\Delta\theta_s$ and $\Delta\theta_{pll(1)}$. The analysis results in this case are similar with that when PLL not exciting oscillation mode. Thus, we will not explore it in this article. Importance is attached on the coupling intensity when the frequency of PLL free response is close to the frequency of system low frequency oscillation. According to resonance mechanism of the system, there is strong coupling between PLL and grid, and resonance occurs in this case. The coupling intensity caused by $\Delta\theta_s$ and $\Delta\theta_{pll(1)}$ is shown as

$$\begin{aligned}\Delta E_{\text{couple2}} &= \frac{\Omega_0}{2} e^{(\alpha+r)t} \Bigg[\Delta\omega_0 - K_i U_s\left(\alpha + r\right) \\ &\quad \times \frac{\Delta\delta_0\left[(r-\alpha)^2 + \beta^2 - \omega_m^2\right]}{A^2 + B^2}\left(2r - 2\alpha\right)\Bigg] \\ &\quad - \frac{\Omega_0}{2} e^{(\alpha+r)t} K_i U_s\left(\alpha + r\right) \frac{\left(\Delta\omega_0 - \alpha\Delta\delta_0\right)}{A^2 + B^2}\left(2r - 2\alpha\right) \end{aligned} \tag{31}$$

where $\Delta E_{\text{couple2}}$ is the new dissipation intensity generated by the coupling between $\Delta\theta_s$ and $\Delta\theta_{pll(1)}$. $\Delta\omega_0$ is the initial value of variation of PLL rotating speed. $\Delta\delta_0$ is the initial value of variation of phase-locked angle.

When PLL exhibits weak damping, i.e., when $0 > \alpha \gg r$, (31) can be simplified as

$$\begin{aligned}\Delta E_{\text{couple2}} &= \frac{\Omega_0}{2} e^{(\alpha+r)t} \\ &\quad \times \left[\Delta\omega_0 - K_i U_s r \frac{\Delta\delta_0\left(r^2 + \beta^2 - \omega_m^2\right)}{\left(r^2 + \beta^2 - \omega_m^2\right)^2 + \left(2r\omega_m\right)^2}\right]. \end{aligned} \tag{32}$$

After PLL is disturbed, $\Delta\omega_0, \Delta\delta_0 < 0$; thus, $\Delta E_{\text{couple2}} < 0$, and the coupling between $\Delta\theta_s$ and $\Delta\theta_{pll(1)}$ will aggravate the damping effect of DFIG. When α and r remain unchanged, adjust K_i so that the frequency of PLL oscillation mode β draws closer to ω_m. According to (32), when $\beta = \omega_0$, $\Delta E_{\text{couple2}}$ reaches the minimum value, and strong resonance will occur between DFIG and system oscillation, which will amplify system low frequency oscillation and make DFIG generates the maximum negative

dissipation intensity and injects dynamic energy to the system, further aggravating system damping level.

The minimum value of $\Delta E_{\text{couple2}}$ can be expressed as

$$\Delta E_{\text{couple2}} = \frac{\Omega_0}{2} e^{(\alpha+r)t} \left[\Delta\omega_0 + \frac{2\Delta\omega_0 - 3\alpha\Delta\delta_0}{4} \right]. \quad (33)$$

It can be seen from (33) that the minimum value of $\Delta E_{\text{couple2}}$ decreases as α increases. Therefore, by increasing the value of K_p and improving the damping level of PLL free response, the minimum value of $\Delta E_{\text{couple2}}$ can be increased, and the diverging effect of DFIG on system oscillation can be weakened.

Based on the above analysis, when PLL excites certain oscillation mode, the coupling between PLL free response $\Delta\theta_{pll(1)}$ and system oscillation $\Delta\theta_s$ will introduce a negative dissipation intensity item. Especially, when the frequencies of $\Delta\theta_{pll(1)}$ and $\Delta\theta_s$ are equal, strong resonance will occur, and if PLL exhibits weak damping, the negative dissipation intensity will reach the minimum value. As the oscillating source, DFIG will continuously inject dynamic energy to the grid, amplifying system oscillation and aggravating system damping level.

Comparison between the dissipation intensities of DFIG in two cases reveals that when PLL does not excite oscillation mode, the coupling between DFIG and grid is relatively small, and the dissipation intensity of DFIG is relatively big; thus, DFIG exhibits positive damping effect on system oscillation. When PLL excites oscillation mode, DFIG and grid are strongly coupled, and the dissipation intensity of DFIG is relatively weak; thus, DFIG may lower system stability level. Based on the above conclusion, the following tuning strategy is put forward.

On the premise of guaranteeing the tracking performance of PLL, PLL parameters are preferentially tuned to be in the interval of $4K_i \leq K_p^2 U_s$ where PLL does not excite oscillation mode. In this interval, modestly decreasing parameter K_p and increasing parameter K_i can improve the dissipation intensity of DFIG on low-frequency oscillation, thus improving system damping level. If PLL parameters cannot meet the conditions of PLL not exciting oscillation mode, PLL parameters can only be tuned to be in the interval of $4K_i > K_p^2 U_s$ where PLL excites oscillation mode. In this case, by increasing parameter K_p, the damping level of PLL can be improved; and by adjusting parameter K_i to render the oscillation frequency of PLL far away from system oscillation frequency, the coupling between DFIG and grid can be weakened; thus, system stability level can be improved.

IV. Simulation Analysis

A. Test System

To verify the correctness of the above DFIG dissipation energy analysis, the hardware-in-the-loop simulation is introduced and the experimental system is shown in Fig. 3. The IEEE 10-machine 39-bus New England system is built in RTDS, as shown in Fig. 31 in Appendix C. Substitute synchronous generator G1 in Area 1 with a wind farm of equal capacity made up of 1.5-MW DFIGs. System parameters can be found in [18].

In order to prove the general applicability of the proposed method, three simulation cases are set in this article, i.e., three phase instantaneous fault, load power fluctuation, and forced oscillation, the parameter setting of which is shown in Table I.

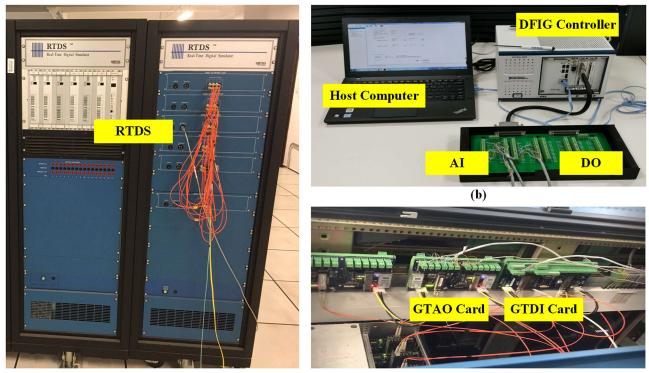

Fig. 3. Experiment platform. (a) RTDS. (b) Experiment platform. (c) Connection diagram between RTDS and DFIG controller.

TABLE I
Setting of Simulation Parameters

Case	Incident	Oscillating generators	Oscillation frequency ω_m (Hz)	Oscillation amplitude Ω_0 (deg)
1	Three phase instantaneous short circuit fault at Bus B31 via 500Ω grounding resistance which lasts for 0.1s.	G10, G4, G6	0.7203	0.3
2	Load at Bus B31 increases by 50%	G8, G2	0.96	0.226
3	Forced oscillation added to the power torque of G2	-	0.5	5.065

Concerning these three simulation cases, the effect of different PLL control parameters on DFIG dissipation intensity is analyzed and compared with hardware-in-the-loop tests, so that the correctness and effectiveness of the above conclusion can be verified.

B. Simulation Verification of Low-Frequency Oscillation Mechanism

1) Case 1:

a) PLL not exciting any oscillation mode: The variation trend of DFIG dissipation intensity corresponding to different control parameters is shown in Fig. 4. It can be seen that DFIG dissipation intensity remains positive in value, and increases as parameter K_i increases, and decreases as parameter K_p increases. Thus, DFIG exerts positive damping effect on system low frequency oscillation.

Variation of the components of DFIG dissipation intensity is further analyzed. When PLL parmeters vary, the variation of coupled dissipation intensity and free dissipation intensity is shown in Fig. 5. It can be seen from Fig. 5(a) that when $K_i < 1.3$, and $0 > r > r_1 + r_2$, $\Delta E_{\text{couple}} < 0$. However, since the free dissipation intensity is the leading component, i.e., $\Delta E_{\text{free}} >$

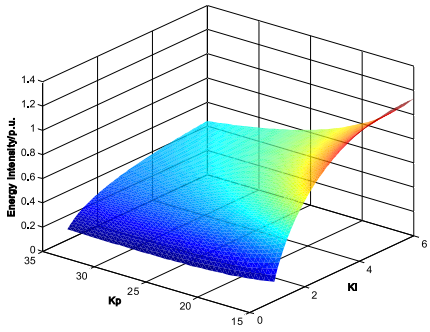

Fig. 4. Variation of DFIG dissipation intensity corresponding to different PLL control parameters when PLL not exciting oscillation mode in case 1.

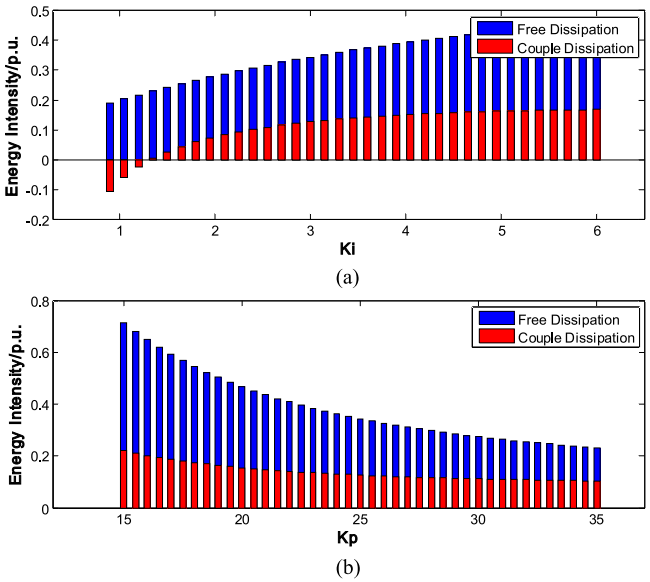

Fig. 5. Variation of free dissipation component and coupled dissipation component corresponding to different PLL control parameters when PLL not exciting oscillation mode in case 1.

ΔE_{couple}, DFIG exhibits positive dissipation effect on the whole. As K_i increases, $\Delta E_{\text{couple}} > 0$, and both ΔE_{free} and ΔE_{couple} increase. In Fig. 5(b), ΔE_{free} and ΔE_{couple} are both above 0, and both decrease as K_p increases. This result is consistent with the conclusion in Section III.

To verify the correctness of the above conclusion, hardware-in-the-loop tests are conducted to compare the power angle curves of PLL and synchronous generators corresponding to four different groups of setting values of control parameters, the results shown in Fig. 6. When PLL does not excite any oscillation mode, the oscillation component in $\Delta\theta_{pll(1)}$ is mainly determined by the forced response, and its oscillation frequency is consistent with the oscillation frequency of system power angle. When K_i increases, the oscillation amplitude of $\Delta\theta_{pll(1)}$ decreases, and the oscillation amplitude of system power angle slightly decreases. When K_p increases, the oscillation amplitude of $\Delta\theta_{pll(1)}$ increases, and the oscillation amplitude of system power angle slightly increases; the damping effect of DFIG on system low frequency oscillation weakens, but the overall damping level is positive.

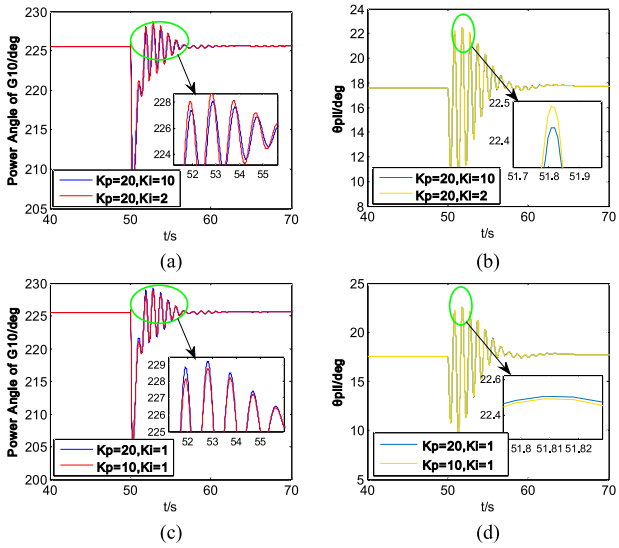

Fig. 6. Oscillation curves of phase-locked angle and G10 power angle corresponding to different PI parameters when PLL not exciting oscillation mode in case 1.

The oscillation curves of DFIG-side current and active power corresponding to three groups of control parameters (i.e., $K_p = 20, K_i = 10, K_p = 20, K_i = 1, K_p = 10, K_i = 1$) are shown in Fig. 7. It can be seen that when K_i increases or K_p decreases, the oscillation amplitude of DFIG active power slightly decreases and system stability is improved. The experimental results are consistent with the theoretical analysis.

b) PLL exciting oscillation mode: The variation of parameter K_i will affect the coupling effect between DFIG and grid. When the damping of PLL is weak ($K_p = 0.1$), the variation of DFIG dissipation intensity corresponding to different values of K_i is shown in Fig. 8.

It can be seen from Fig. 8(a) that, as K_i keeps increasing, the oscillation frequency of PLL gradually approaches the electromechanical oscillation frequency 0.7201 Hz, DFIG dissipation intensity gradually decreases and turns from positive to negative. In the vicinity of electromechanical oscillation frequency, DFIG dissipation intensity reaches the minimum value. Two leading components of DFIG dissipation intensity are shown in Fig. 8(b). It can be seen that the free dissipation intensity gradually decreases as K_{i} increases, and the coupled dissipation intensity reaches the minimum value at the electromechanical oscillation frequency, when DFIG is strongly coupled with the grid and continuously injects dynamic energy to the grid, which will amplify system oscillation and aggravate system damping.

The variation of the minimum value of DFIG dissipation intensity with K_p is shown in Fig. 9. When K_p is relatively small, and PLL exhibits weak damping, DFIG dissipation intensity is negative. As K_p gradually increases, the damping of PLL oscillation mode strengthens, and DFIG dissipation intensity gradually increases to positive value. The components of DFIG dissipation intensity are shown in Fig. 9(b). It can be seen that the coupled dissipation intensity and free dissipation intensity both decrease as K_p increases. When $K_p > 0.3$, the sum of two components is above 0; thus, although the resonance between

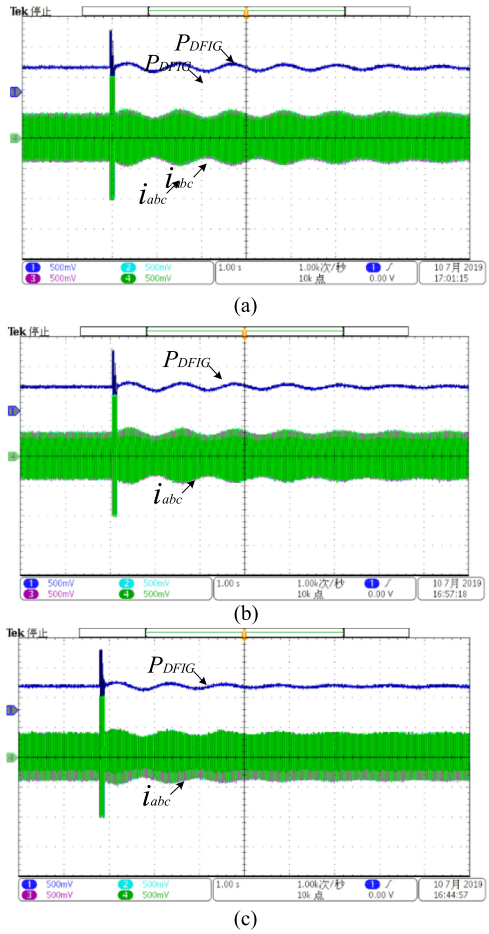

Fig. 7. Oscillation curves of DFIG-side current and active power corresponding to three groups of control parameters when PLL not exciting oscillation mode in case 1.

DFIG and grid will amplify system low frequency oscillation, DFIG still exhibits positive damping effect on system oscillation and will not cause the system to diverge.

To verify the correctness of the above conclusion, hardware-in-the-loop tests are conducted concerning six groups of control parameter settings, i.e., $K_i = 20$ with $K_p = 0.1$, 0.3, 0.6 and $K_p = 0.1$ with $K_i = 17$, 20, 26. The variation curves of phase-locked angle and G10 power angle are shown in Figs. 10 and 11, respectively. It can be seen that when $K_i = 20$, $K_p = 0.1$, the coupling between DIFG and grid generates resonance, and PLL exhibits weak damping; thus, the system oscillates to instability. As K_p increases, the oscillation of system and PLL gradually attenuate and converge to stability. When PLL remains at weak damping level, by increasing K_i to make β gradually approach ω_m, the resonance between DFIG and grid occurs and the angle of PLL oscillates with equal amplitude. The oscillation of power angle of G10 converges in initial stage. However, with DFIG continuously injecting oscillation component, the power angle oscillation develops into an equal amplitude oscillation, causing the system to go unstable. When β is far from ω_m, the coupling between DFIG and grid is weak, and system oscillation will converge. This simulation result is consistent with the above theoretical analysis.

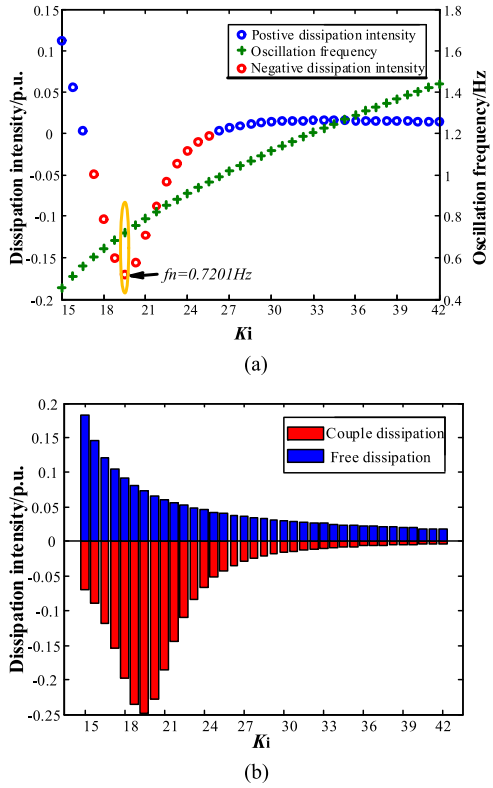

Fig. 8. DFIG dissipation intensity and its free and forced components corresponding to different values of K_i when PLL exciting oscillation mode in case 1. (a) Variation of dissipation intensity and oscillation frequency with K_i. (b) Variation of forced dissipation intensity and free dissipation intensity with K_i.

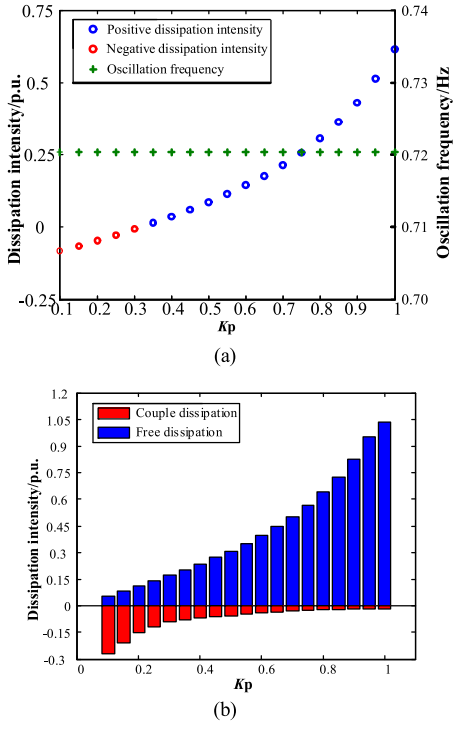

Fig. 9. DFIG dissipation intensity and its free and forced components corresponding to different values of K_p when PLL exciting oscillation mode in case 1. (a) Variation of dissipation intensity and oscillation frequency with K_p. (b) Variation of forced dissipation intensity and free dissipation intensity with K_p.

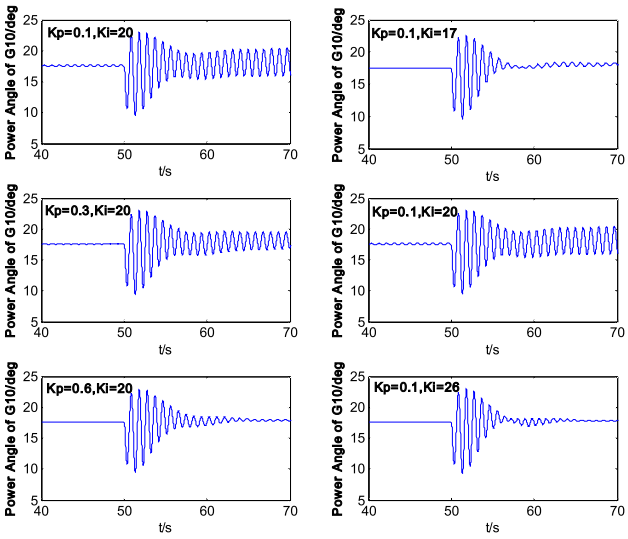

Fig. 10. Oscillation curves of G10 power angle corresponding to different PLL control parameters when PLL exciting oscillation mode in case 1.

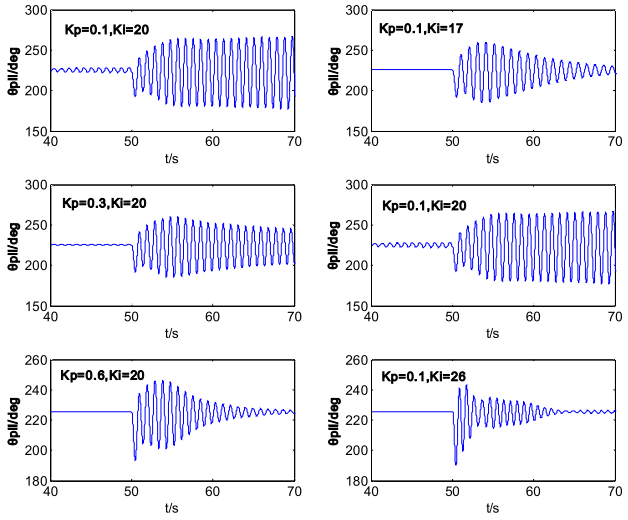

Fig. 11. Oscillation curves of phase-locked angle corresponding to different PLL control parameters when PLL exciting oscillation mode in case 1.

The variation curves of DFIG-side current and active power corresponding to the six groups of control parameters are shown in Fig. 12. It can be seen that as K_p increases, the oscillation of DFIG active power gradually attenuate and converge to stability. When PLL remains at weak damping level, by increasing K_i to make β gradually approach ω_m, the resonance between DFIG and grid occurs and DFIG active power oscillates to divergence, which leads to the instability of system. The experimental results are consistent with the theoretical analysis.

2) Case 2: Low frequency oscillation caused by the fluctuation of load power is essentially similar to Case 1; both are relative oscillation between power angles caused by system disturbance, only different in oscillation mode and parameters. Thus, Case 2 can be analyzed in the same way as Case 1, which is not repeated here. The simulation results of Case 2 are as follows.

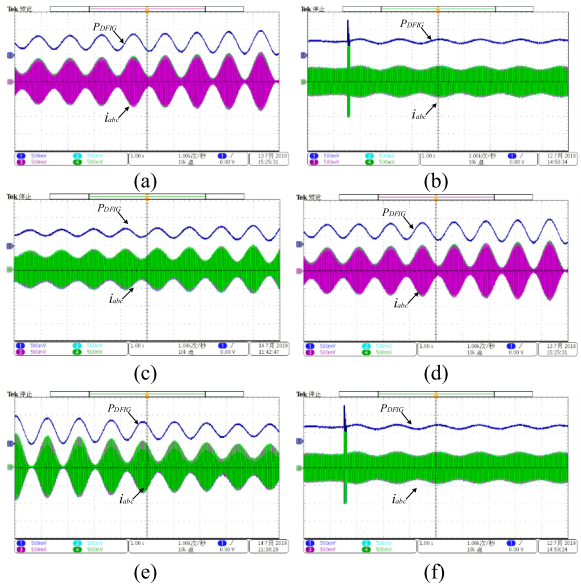

Fig. 12. Oscillation curves of DFIG-side current and active power corresponding to three groups of control parameters when PLL exciting oscillation mode in case 1.

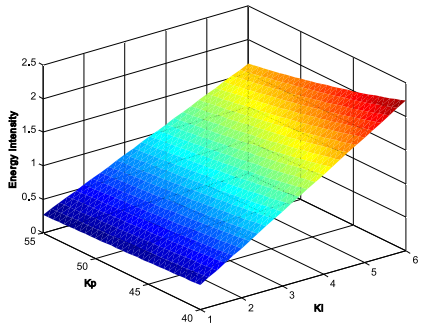

Fig. 13. Variation of DFIG dissipation intensity corresponding to different PLL control parameters when PLL not exciting oscillation mode in case 2.

a) PLL not exciting any oscillation mode: The variation trend of DFIG dissipation intensity corresponding to different control parameters is shown in Fig. 13. It can be seen that DFIG dissipation intensity is constantly positive, increases as K_i increases, and decreases as K_p increases. Thus, in this case, DFIG has positive damping effect on system oscillation.

When PLL control parmeters vary, the variation of coupled dissipation intensity and free dissipation intensity is shown in Fig. 14. It can be seen that both coupled dissipation intensity and free dissipation intensity are constantly above 0, and coupled dissipation intensity is the leading component. This is because in this setting of parameters, the forced response of PLL is much bigger than the free response. Both components of DFIG dissipation intensity increase as K_i increases and decrease as K_p increases. Such simulation result is consistent with theoretical analyis.

The oscillation curves of phase-locked angle and G8 power angle corresponding to four groups of control parameters (i.e., $K_p = 45$ with $K_i = 2$, 4 and $K_i = 4$ with $K_p = 30$, 50) are shown in Fig. 15. It can be seen that, in this case, the forced

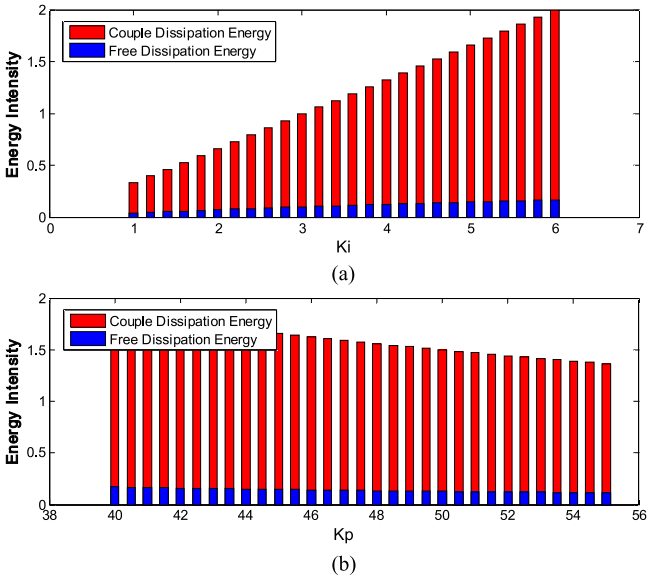

Fig. 14. Variation of free dissipation component and coupled dissipation component corresponding to different PLL control parameters when PLL not exciting oscillation mode in case 2.

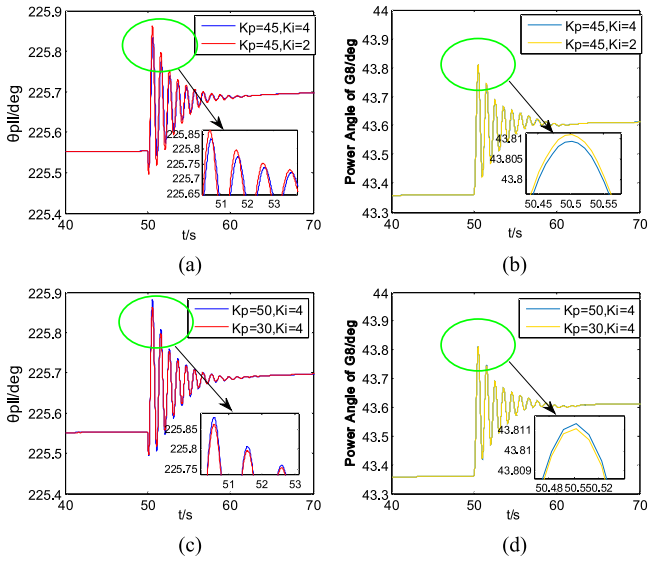

Fig. 15. Oscillation curves of phase-locked angle and G8 power angle corresponding to different PI parameters when PLL not exciting oscillation mode in case 2.

response is leading the response curves of phase-locked angle, the oscillation trend of which is similar to that of system oscillation. When K_i increases, the damping of DFIG increases, PLL oscillation amplitude drops, and the oscillation of G8 power angle also slightly converges. When K_p increases, the damping of DFIG decreases, the oscillation amplitudes of PLL and G8 power angle both increase, but since the overall damping is still positive, the system finally converges to stability. Such hardware-in-the-loop tests results verify the correctness and effectiveness of the above analysis.

The oscillation curves of DFIG-side current and active power corresponding to three groups of control parameters (i.e., $K_p = 50$, $K_i = 2$, $K_p = 30$, $K_i = 2$, $K_p = 3$, $K_i = 4$) are shown in Fig. 16. It can be seen that when K_i increases or K_p decreases, the oscillation attenuation of DFIG-side current and active power increases gradually, which is consistent with the theoretical analysis.

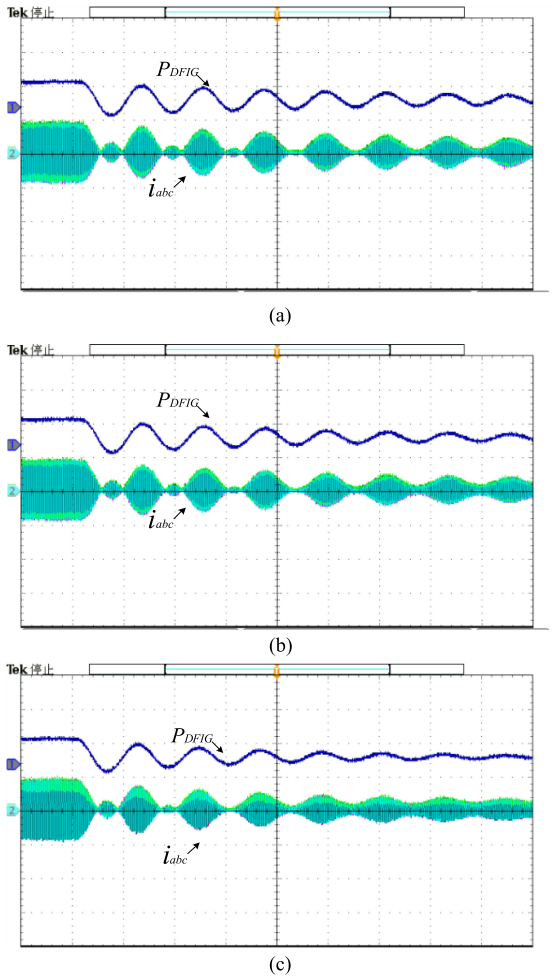

Fig. 16. The oscillation curves of DFIG-side current and active power corresponding to three groups of control parameters when PLL not exciting oscillation mode in case 2. (a) $K_p = 50$, $K_i = 2$. (b) $K_p = 30$, $K_i = 2$. (c) $K_p = 30$, $K_i = 4$.

b) PLL exciting oscillation mode: The variation trend of DFIG dissipation intensity corresponding to different control parameters is shown in Fig. 17. It can be seen that when $K_i = 46$, DFIG dissipation intensity reaches the minimum value, and this minimum value increases as K_p increases.

The variation of DFIG coupled dissipation intensity and free dissipation intensity are shown in Fig. 18. It can be seen from Fig. 18(a) that the free dissipation intensity is constantly positive, while the coupled dissipation intensity is negative and reaches its minimum value when $K_i = 46$. Since the forced response of PLL is bigger than the free response in this case, the coupled dissipation intensity is the leading component. The sum of two components is negative; thus, DFIG continuously injects dynamic energy to the system, aggravating system damping level. In Fig. 18(b), as K_p increases, the free dissipation intensity and coupled dissipation intensity both increase. When $K_p > 0.56$,

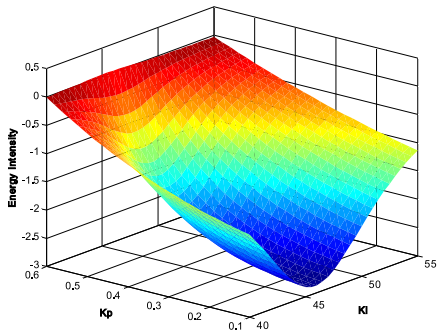

Fig. 17. Variation of DFIG dissipation intensity corresponding to different PLL control parameters when PLL exciting oscillation mode in case 2.

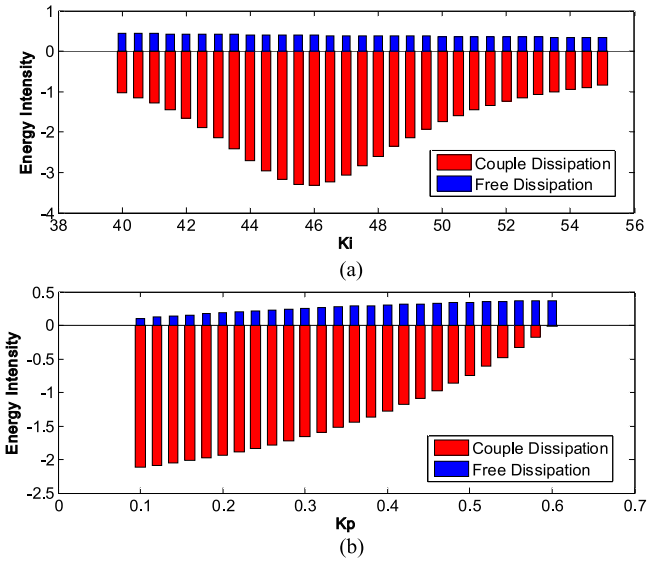

Fig. 18. Variation of free dissipation component and coupled dissipation component corresponding to different PLL control parameters when PLL exciting oscillation mode in case 2.

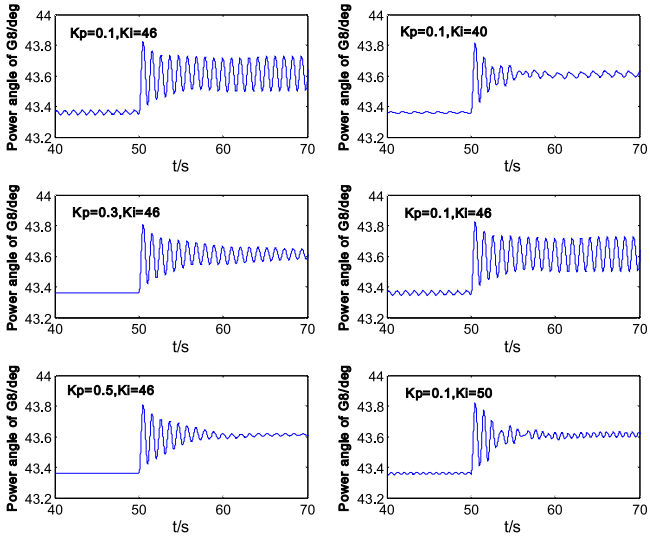

Fig. 19. Oscillation curves of G8 power angle corresponding to different PLL control parameters when PLL exciting oscillation mode in case 2.

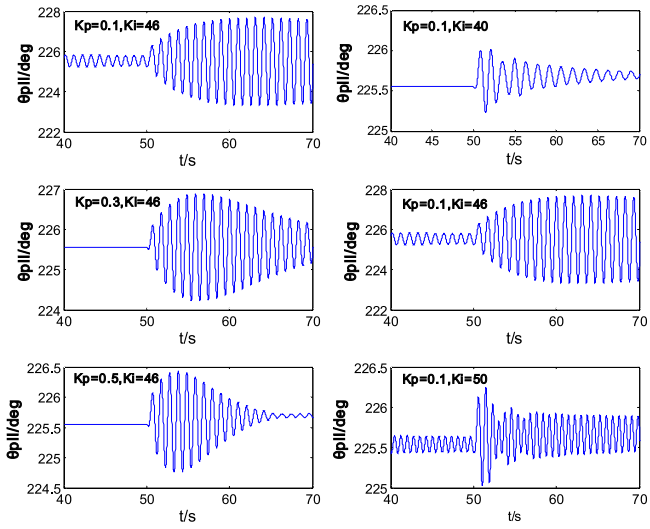

Fig. 20. Oscillation curves of phase-locked angle corresponding to different PLL control parameters when PLL exciting oscillation mode in case 2.

the sum of two components turns positive; thus, the damping of DFIG turns positive, and the system turns from unstable state to stable state.

Hardware-in-the-loop tests are conducted concerning six groups of parameters, i.e., $K_i = 46$ with $K_p = 0.1, 0.3, 0.5$ and $K_p = 0.1$ with $K_i = 40, 46, 50$, and the oscillation curves of G8 power angle and phase-locked angle are shown in Figs. 19 and 20 respectively. When $K_i = 46$, and PLL exhibits weak damping, the resonance between DFIG and grid causes constant-amplitude oscillation in system side and PLL. As K_p keeps increasing, the damping effect of DFIG on the resonance gradually increases; thus, the oscillation gradually converges. By adjusting the value of K_i, the distance between β and ω_m can be adjusted. The closer β is to ω_m, the stronger the resonance between DFIG and grid is, and the more probably PLL will oscillate to divergence and cause system to oscillate to instability. When β is far from ω_m, the coupling between DFIG and grid is weak; thus, the resonance is weakened, and the damping effect of DFIG on system oscillation is strengthened. This simulation result is consistent with the above theoretical analysis.

The oscillation curves of DFIG-side current and active power corresponding to the six groups of control parameters are shown in Fig. 21. Increasing K_p or adjusting K_i parameters to make PLL oscillation frequency far away from system oscillation frequency is beneficial to increase the damping effect of DFIG on system oscillation and enhancing system stability level.

3) Case 3:

a) PLL not exciting any oscillation mode: If forced oscillation occurs in the system, DFIG will continuously absorb oscillation energy from the system. When PLL does not excite any oscillation mode, the variation of DFIG dissipation intensity corresponding to different PLL parameters is shown in Fig. 22. It can be seen that DFIG dissipation intensity is constantly positive with similar variation pattern to the former two cases.

As PLL control parameters vary, the variation of free dissipation intensity and coupled dissipation intensity is shown

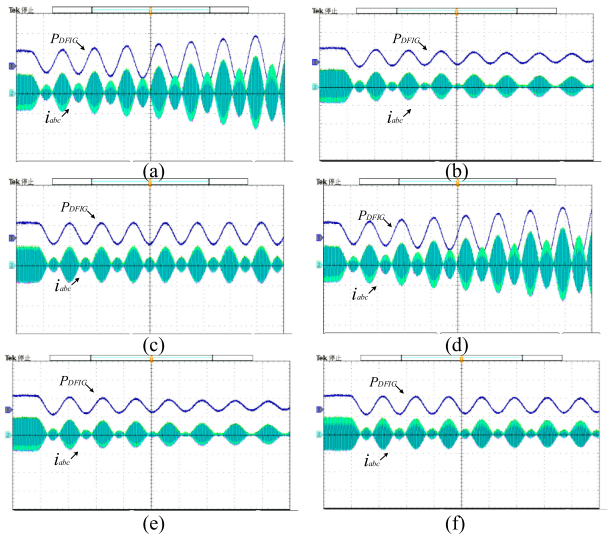

Fig. 21. The Oscillation curves of DFIG-side current and active power corresponding to three groups of control parameters when PLL exciting oscillation mode in case 2. (a) $K_p = 0.1$, $K_i = 46$. (b) $K_p = 0.3$, $K_i = 46$. (c) $K_p = 0.5$, $K_i = 46$. (d) $K_p = 0.1$, $K_i = 40$. (e) $K_p = 0.1$, $K_i = 46$. (f) $K_p = 0.1$, $K_i = 50$.

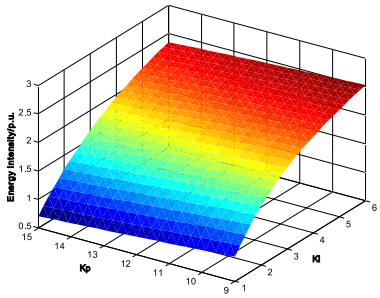

Fig. 22. Variation of DFIG dissipation intensity corresponding to different PLL control parameters when PLL not exciting oscillation mode in case 3.

in Fig. 23. It can be seen that the free dissipation intensity and coupled dissipation intensity are both positive, with free dissipation being the leading component, and both components increase as K_i increases and decrease as K_p increases.

Hardware-in-the-loop tests of phase-locked angle and power angle of voltage at Bus39 corresponding to different PI parameters are shown in Fig. 24. It can be seen that when K_i increases, the oscillation amplitude of phase-locked angle decreases; when K_p increases, the oscillation amplitude of phase-locked angle increases. The phase angle of voltage at Bus39 has similar variation pattern, due to the relatively weak coupling between DFIG and grid, only with smaller variation amplitude.

The oscillation curves of DFIG-side current and active power corresponding to three groups of control parameters (i.e., $K_p = 15$, $K_i = 1$, $K_p = 10$, $K_i = 1$, $K_p = 10$, $K_i = 3$) are shown in Fig. 25. It can be seen that when K_i increases or K_p decreases, equal-amplitude oscillation amplitude is reduced and system stability level is enhanced. The test result is consistent with the theoretical analysis.

b) PLL exciting oscillation mode: As β draws closer to ω_m, resonance will occur between PLL and the system. As the

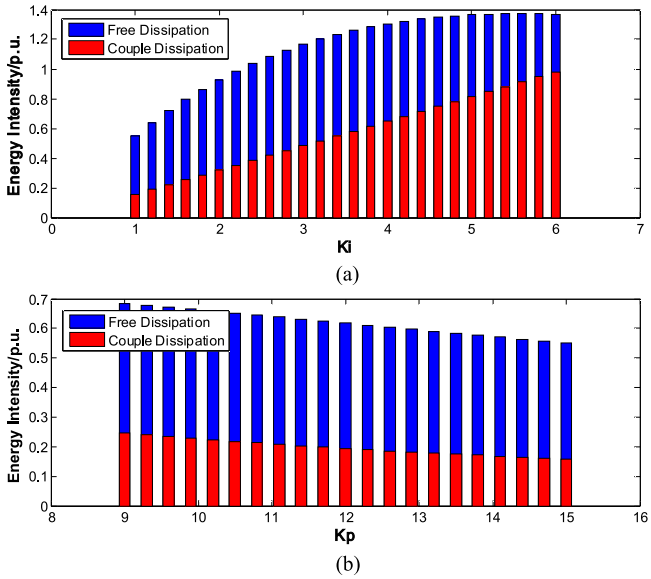

Fig. 23. Variation of free dissipation component and coupled dissipation component corresponding to different PLL control parameters when PLL not exciting oscillation mode in case 3.

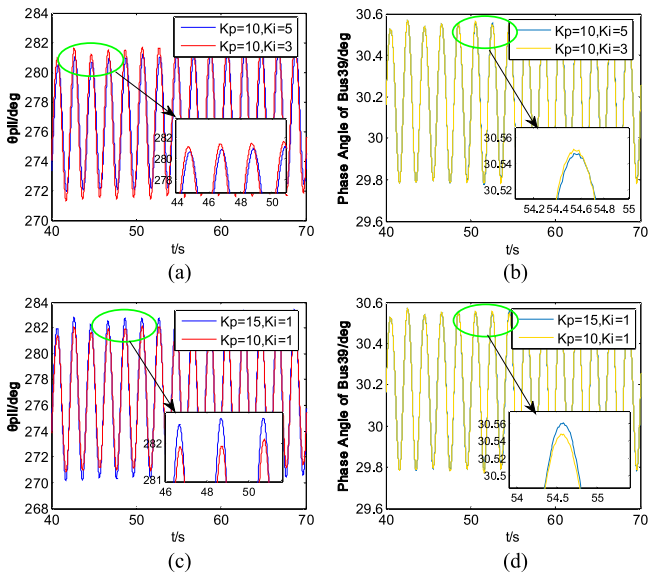

Fig. 24. Oscillation curves of phase-locked angle and power angle of voltage at Bus39 corresponding to different PI parameters when PLL not exciting oscillation mode in case 3.

oscillating source, DFIG will inject oscillation energy to the system; thus, DFIG dissipation intensity will be negative and will reach its minimum value when $\beta = \omega_m$. As PLL control parameters vary, the variation of DFIG dissipation intensity is shown in Fig. 26.

Fig. 27 depicts the variation of free dissipation intensity and coupled dissipation intensity corresponding to different PLL control parameters. It can be seen that, as β draws closer to ω_m, the coupled dissipation intensity decreases rapidly and turns negative; thus, DFIG injects oscillation energy to the system, and the injected oscillation energy reaches the maximum value

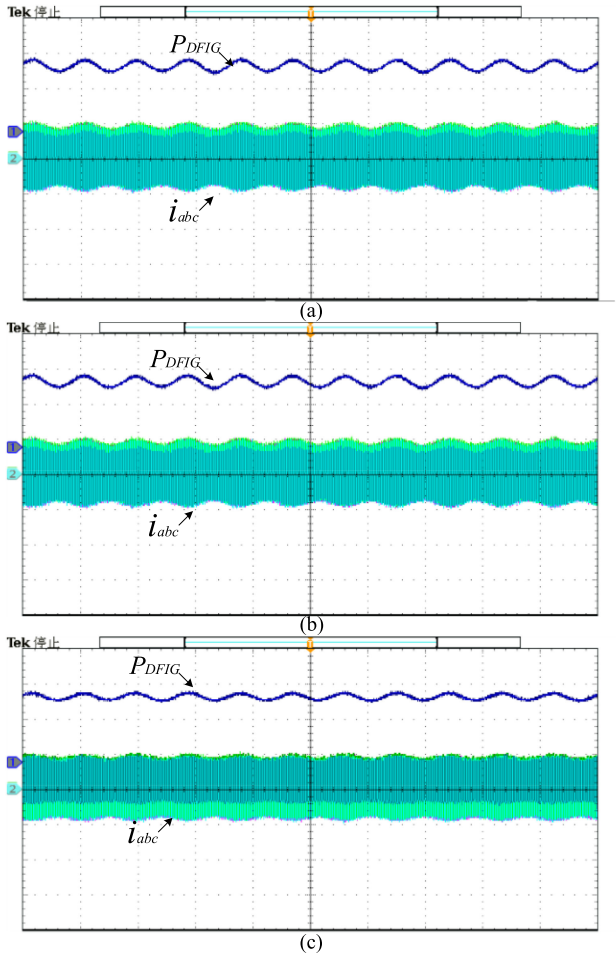

Fig. 25. Oscillation curves of DFIG-side current and active power corresponding to three groups of control parameters when PLL not exciting oscillation mode in case 3. (a) $K_p = 15$, $K_i = 1$. (b) $K_p = 10$, $K_i = 1$. (c) $K_p = 10$, $K_i = 3$.

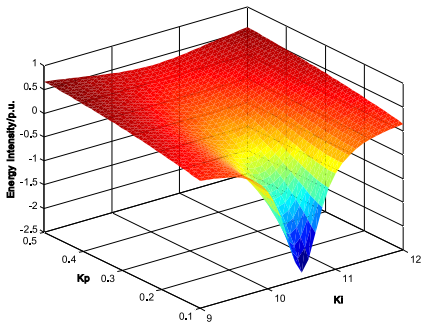

Fig. 26. Variation of DFIG dissipation intensity corresponding to different PLL control parameters when PLL exciting oscillation mode in case 3.

when $\beta = \omega_m$. This maximum value keeps increasing as K_p increases.

In this case, the hardware-in-the-loop tests curves of phase-locked angle are shown in Fig. 28. It can be seen that as K_p increases, the oscillation amplitude of phase-locked angle gradually decreases. When $K_i = 10.6$, i.e., when the frequency of PLL oscillation mode is equal to system oscillation frequency, resonance occurs between DFIG and the system, which amplifies

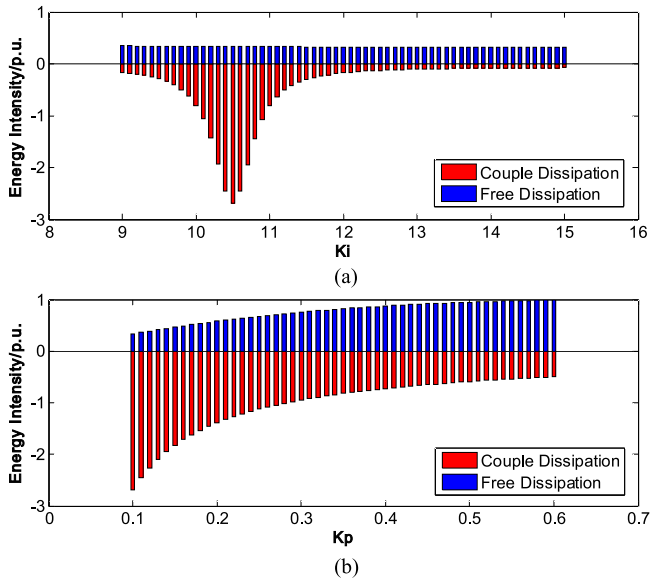

Fig. 27. Variation of free dissipation component and coupled dissipation component corresponding to different PLL control parameters when PLL exciting oscillation mode in case 3.

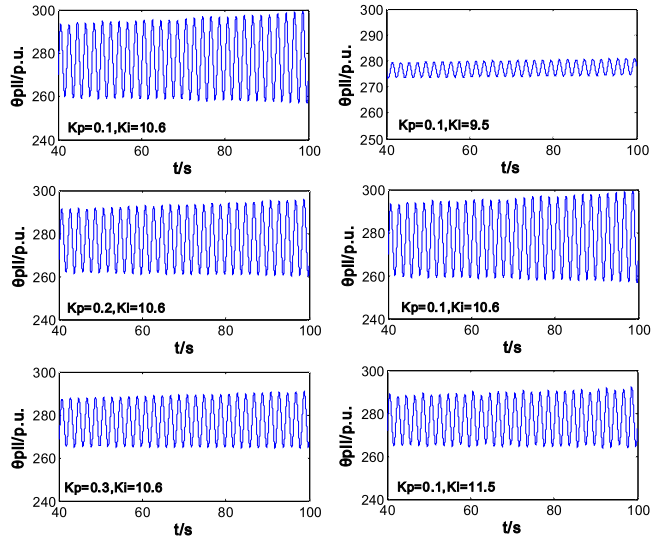

Fig. 28. Oscillation curves of phase-locked angle corresponding to different PLL control parameters when PLL exciting oscillation mode in case 3.

system oscillation, and the damping of DFIG turns negative. Thus, the above theoretical analysis result is verified.

The oscillation curves of DFIG-side current and active power corresponding to the six groups of control parameters are shown in Fig. 29. Increasing K_p or adjusting K_i parameters to make PLL oscillation frequency far away from system oscillation frequency is beneficial to reduce equal-amplitude oscillation amplitude, increase the damping effect of DFIG on system oscillation and enhancing system stability level.

C. Comparison With Eigenvalue Analysis Method

To verify the applicability and effectiveness of the proposed energy method in analyzing the stability of low-freqeuncy oscillation, the consistency of the participation degree of DFIG in

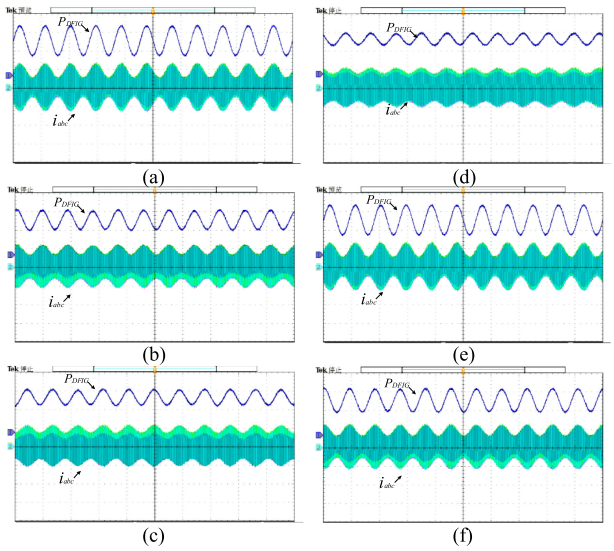

Fig. 29. Oscillation curves of DFIG-side current and active power corresponding to three groups of control parameters when PLL exciting oscillation mode in case 3. (a) $K_p = 0.1$, $K_i = 10.6$. (b) $K_p = 0.2$, $K_i = 10.6$. (c) $K_p = 0.3$, $K_i = 10.6$. (d) $K_p = 0.1$, $K_i = 9.5$. (e) $K_p = 0.1$, $K_i = 10.6$. (f) $K_p = 0.1$, $K_i = 11.5$.

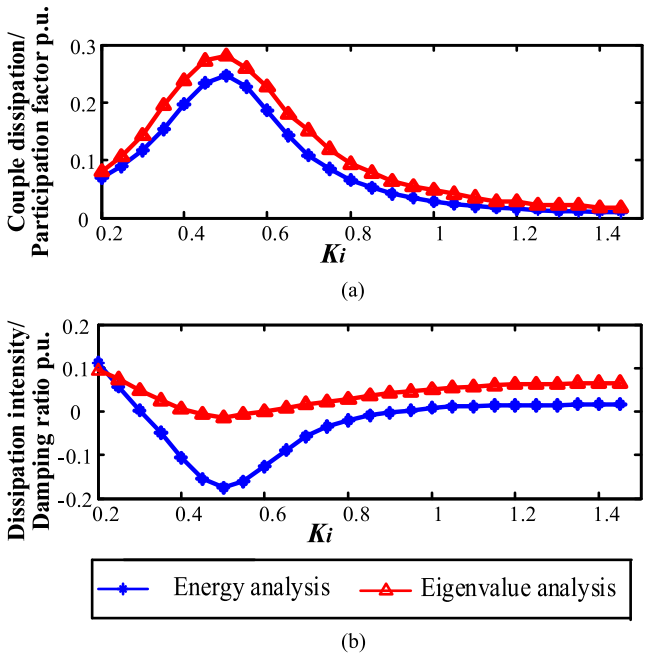

Fig. 30. Comparison between energy analysis result and eigenvalue calculation result. (a) Comparison between system damping ratio and coupled dissipation intensity. (b) Participation factor and forced dissipation intensity.

electromechanical oscillation and the effect of DFIG on system damping obtained with the energy method and eigenvalue analysis method [19] is analyzed. Take Case 1 for example. The case, weak damping with PLL exciting oscillation mode, is analyzed in detail. The parameter setting is the same as the one shown in Figs. 8 and 9. The comparison results of the other parameters are similar and shown in Appendix D.

In order to make the comparison more obvious, the absolute value of coupled dissipation intensity is used, which characterizes the degree of coupling between DFIG and grid. The variation curves of PLL participation factor and the absolute value of coupled dissipation intensity are shown in Fig. 30(a). It can be seen that the variation trends of two curves are almost the same. When $K_i = 0.5$, the participation degree of DFIG in system electromechanical oscillation reaches the maximum. Comparison between DFIG dissipation intensity and system damping ratio is shown in Fig. 30(b). It can be seen that both reach the lowest point when the frequency of PLL excited oscillation is equal to the frequency of system electromechanical oscillation. This is consisent with the analysis result in Section III.

Based on the above analysis, the results of eigenvalue calculation and energy analysis are consistent; thus, the proposed energy method can be effectively applied in analyzing low-frequency oscillation of the DFIG-integrated system. Meanwhile, according to the above comparison, the eigenvalue method can only reach the conclusion that when PLL oscillation mode is coupled with system electromechanical oscillation mode. However, it cannot accurately analyze the damping level of DFIG itself and how DFIG-grid coupling causes the system to oscillate to instability. As for the energy method, the mechanism of how DFIG-grid coupling affects system low-frequency oscillation is further illustrated, with the conclusion that the energy interaction between DFIG and grid caused by PLL will weaken the damping of DFIG itself. When DFIG is strongly coupled with the grid, the damping of DFIG will rapidly deteriorate, and DFIG will continuously inject dynamic energy to the grid, causing the system to oscillate to instability.

V. Conclusion

A method to analyze the low-freqeuncy oscillation of the system with DFIG integration based on the dissipation energy is proposed in this article. By constructing the model of dissipation energy of DFIG with PLL, the interaction between DFIG and power grid is analyzed, and the mechanism of how DFIG-integrated system goes unstable from low-freqeuncy oscillation is illustrated from the perspective of energy. Main conclusions are as follows.

1) The dynamic characteristics of PLL cause DFIG to be coupled with the grid, which generates new dissipation energy composed of free dissipation energy and DFIG-grid coupled dissipation energy. Free dissipation energy is the dissipation effect of DFIG on the dynamic energy generated by the free response of PLL, and its intensity represents the immanent damping level of DFIG. Coupled dissipation energy is the dissipation of dynamic energy generated by the coupling between DFIG and grid, and its intensity represents DFIG-grid coupling degree. If the positive damping of DFIG free dissipation cannot offset the negative damping effect generated by DFIG-grid coupling, DFIG will go unstable and cause system electromechanical oscillation to diverge, aggravating system damping level.

2) When PLL does not excite any oscillation mode, the free dissipation intensity is the leading component. Although the coupling dissipation intensity maybe negative when parameter K_i decreases, the total intensity keeps positive and DFIG exhibit positive damping on the oscillation. Both of the dissipation intensity increase as K_i increases and decrease as K_p increases.
3) When PLL excites some oscillation mode, the coupling between PLL free response and system oscillation will introduce a negative dissipation intensity item. When the two frequencies come to be equal, strong resonance will occur, and if PLL exhibits weak damping, the negative dissipation intensity will reach the minimum value. As the oscillating source, DFIG will continuously inject dynamic energy to the grid, amplifying system oscillation and aggravating system damping level.
4) The proposed method does not require the state variables of all generators in the system to be obtained. From the perspective of DFIG alone, through the DFIG-grid coupled dissipation intensity, the degree of coupling between DFIG and grid is accurately quantified, the damping effect of DFIG-grid coupling on DFIG is evaluated, and the physical process of how the energy interaction between DFIG and grid causes system oscillation to diverge when there is strong coupling between DFIG and grid is revealed.

APPENDIX A

When the eigenvalue of (18) is real number, the general solution corresponds to PLL not exciting oscillation mode; thus, the free response of PLL can be expressed as

$$\Delta\theta_{\mathrm{pll}(1)} = C_1 e^{\alpha_1 t} + C_2 e^{\alpha_2 t} \tag{A-1}$$

where α_1 and α_2 are two eigenvalues of (14), and r_1, $r_2 < 0$ because both K_p and K_i are above 0. $C_1 = \Delta\theta_0 - \frac{\Delta\omega_0 - \Delta\theta_0 / r_1}{r_2 - r_1}$ and $C_2 = \frac{\Delta\omega_0 - \Delta\theta_0 / r_1}{r_2 - r_1}$ are coefficients determined by the initial values of the phase-locked angle and rotating speed.

When the eigenvalue of (14) is imaginary number, the dynamic of PLL will excite oscillation mode of its own. The dynamic of PLL is expressed as

$$\Delta\theta_{\mathrm{pll}(1)} = e^{\alpha t} \left(C_1 \cos \beta t + C_2 \sin \beta t\right) \tag{A-2}$$

where β is the oscillation mode of PLL, and α is the attenuation coefficient of this oscillation mode. $C_1 = \Delta\theta_0$ and $C_2 = \frac{\Delta\omega_0 - \alpha\Delta\theta_0}{\beta}$ are coefficients determined by the initial values of the phase-locked angle and rotating speed.

APPENDIX B

$$b = \frac{\Omega_0 * \left(r^2 - \omega_m^2 + K_p U_s r + K_i U_s\right)}{\left(2\omega_m r + K_p U_s \omega_m\right)^2 + \left(r^2 - \omega_m^2 + K_p U_s r + K_i U_s\right)^2} \tag{B-1}$$

$$d = \frac{\Omega_0 \left(2\omega_m r + K_p U_s \omega_m\right)}{\left(2\omega_m r + K_p U_s \omega_m\right)^2 + \left(r^2 - \omega_m^2 + K_p U_s r + K_i U_s\right)^2}. \tag{B-2}$$

APPENDIX C

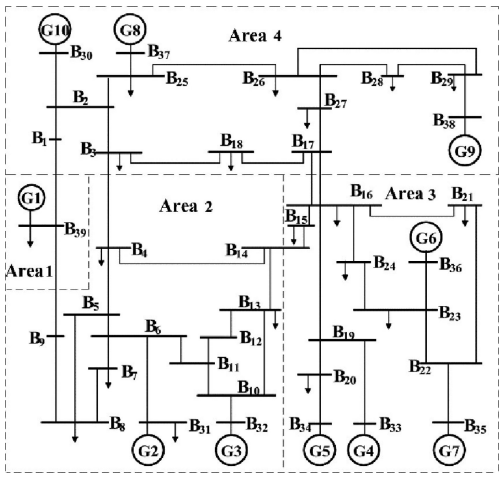

Fig. 31. Diagram of 10-machine 39-bus system.

APPENDIX D

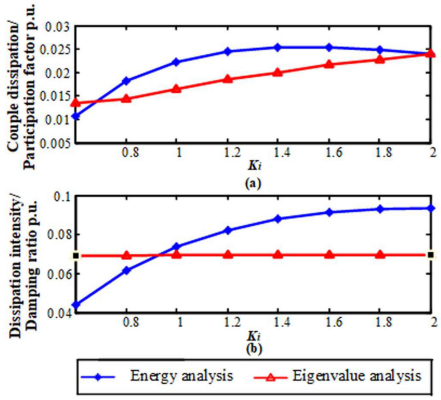

Fig. 32. Comparison between energy analysis result and eigenvalue calculation result (PLL not exciting oscillation mode). (a) Comparison between system damping ratio and coupled dissipation intensity. (b) Participation factor and forced dissipation intensity.

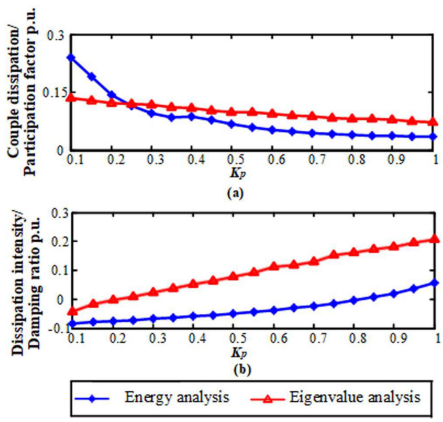

Fig. 33. Comparison between energy analysis method and eigenvalue calculation method (PLL exciting oscillation mode with weak damping). (a) Comparison between system damping ratio and coupled dissipation intensity. (b) Participation factor and forced dissipation intensity.

REFERENCES

[1] Y. Mishra, S. Mishra, F. Li, Z. Y. Dong, and R. C. Bansal, "Small-signal stability analysis of a DFIG-based wind power system under different modes of operation," *IEEE Trans. Energy Convers.*, vol. 24, no. 4, pp. 972–982, Dec. 2009.

[2] J. Fang, H. Li, Y. Tang, and F. Blaabjerg, "Distributed power system virtual inertia implemented by grid-connected power converters," *IEEE Trans. Power Electron.*, vol. 33, no. 10, pp. 8488–8499, Oct. 2018.

[3] G. Durga, V. Vittal, and T. Habour, "Impact of increased penetration of DFIG based wind turbine generators on transient and small signal stability of power systems," *IEEE Trans. Power Syst.*, vol. 24, no. 3, pp. 1426–1434, Aug. 2009.

[4] E. Mohamed, K. L. Lo, and O. Anaya-Lara, "Impacts of high penetration of DFIG wind turbines on rotor angle stability of power systems," *IEEE Trans. Sustain. Energy*, vol. 6, no. 3, pp. 759–766, Apr. 2015.

[5] S. Bu, W. Du, and H. Wang, "Investigation on probabilistic small-signal stability of power systems as affected by offshore wind generation," *IEEE Trans. Power Syst.*, vol. 30, no. 5, pp. 2479–2486, Sep. 2015.

[6] W. Du, X. Chen, and H. Wang, "Power system electromechanical oscillation modes as affected by dynamic interactions from grid-connected PMSGs for wind power generation," *IEEE Trans. Sustain. Energy*, vol. 8, no. 3, pp. 1301–1312, Jul. 2017.

[7] J. Ma, Y. Qiu, Y. Li, W. Zhang, Z. Song, and J. S. Thorp, "Research on the impact of DFIG virtual inertia control on power system small-signal stability considering the phase-locked loop," *IEEE Trans. Power Syst.*, vol. 32, no. 3, pp. 2094–2105, May 2017.

[8] H. Geng, X. Xi, and G. Yang, "Small-signal stability of power system integrated with ancillary-controlled large-scale DFIG-based wind farm," *IET Renewable Power Gener.*, vol. 11, no. 8, pp. 1191–1198, 2017.

[9] W. Du, J. Bi, J. Cao, and H. F. Wang, "A method to examine the impact of grid connection of the DFIGs on power system electromechanical oscillation modes," *IEEE Trans. Power Syst.*, vol. 31, no. 5, pp. 3775–3784, Sep. 2016.

[10] W. Du, X. Chen, and H. Wang, "Impact of dynamic interactions introduced by DFIGs on power system electromechanical oscillation modes," *IEEE Trans. Power Syst.*, vol. 32, no. 6, pp. 4954–4967, Nov. 2017.

[11] W. Du *et al.*, "Impact of grid connection of large-scale wind farms on power system small-signal angular stability," *CSEE J. Power Energy Syst.*, vol. 1, no. 2, pp. 83–89, 2015.

[12] W. Lu *et al.*, "Power system oscillation analysis and oscillation source location based on WAMS Part 2: Method of torques decomposition," *Proc. CSEE*, vol. 33, no. 25, pp. 41–46, 2013.

[13] A. Mohammadreza and F. Ehab, "Implementing virtual inertia in DFIG-based wind power generation," *IEEE Trans. Power Syst.*, vol. 28, no. 2, pp. 1373–1384, May 2013.

[14] S. Chondrogiannis and M. Barnes, "Stability of doubly-fed induction generator under stator voltage orientated vector control," *IET Renewable Power Gener.*, vol. 2, no. 3, pp. 170–180, 2018.

[15] J. Ma *et al.*, "Model order reduction analysis of DFIG integration on the power system small-signal stability considering the virtual inertia control," *IET Gener. Transmiss. Distrib.*, vol. 11, no. 16, pp. 4087–4095, 2017.

[16] W. Du, X. Chen, and H. Wang, "Parameter tuning of the PLL to consider the effect on power system small-signal angular stability," *IET Renewable Power Gener.*, vol. 12, no. 1, pp. 1–8, 2018.

[17] C. Lv, W. Du, and T. Littler, "Damping torque analysis of power systems with DFIG wind turbine generators," in *Proc. Int. Conf. Renewable Power Gener.*, pp. 1–6, 2016.

[18] M. A. Pai, *Energy Function Analysis for Power System Stability*. Boston, MA, USA: Kluwer Academic, 1989.

[19] Z. Wang, S. Chen, and F. Liu, "Impact of DFIG with phase lock loop dynamics on power systems small signal stability," in *Proc. PES Gen. Meeting Conf. Expo.*, pp. 1–5, 2014.

Yaqi Shen was born in Jiangsu Province, China. She is currently working toward the doctoral degree in the School of Electrical and Electronic Engineering, North China Electric Power University, Beijing, China.

Her interests mainly include power system stability analysis and control.

Jing Ma (S'06–M'08–SM'17) received the B.S. and Ph.D. degrees from North China Electric Power University, Beijing, China, in 2003 and 2008, respectively.

He was a Visiting Research Scholar with the Bradley Department of Electrical and Computer Engineering, Virginia Polytechnic Institute and State University, Blacksburg, VA, USA, from 2008 to 2009. He is currently a Professor with the School of Electrical and Electronic Engineering, North China Electric Power University. His major research interests include power system stability and control.

Letian Wang is currently working toward the doctoral degree in the School of Electrical and Electronic Engineering, North China Electric Power University, Beijing, China.

His research interests mainly include power system stability analysis and control.